

Subgrid vertical
velocity and cloud
microphysics

J. Tonttila et al.

Monte Carlo-based subgrid parameterization of vertical velocity and stratiform cloud microphysics in ECHAM5.5-HAM2

J. Tonttila^{1,2}, P. Räisänen¹, and H. Järvinen²

¹Finnish Meteorological Institute, P.O. Box 503, 00101, Helsinki, Finland

²Division of Atmospheric Sciences, Department of Physics, University of Helsinki, 00014, Helsinki, Finland

Received: 4 February 2013 – Accepted: 12 February 2013 – Published: 27 February 2013

Correspondence to: J. Tonttila (juha.tonttila@fmi.fi)

Published by Copernicus Publications on behalf of the European Geosciences Union.

Title Page

Abstract

Introduction

Conclusions

References

Tables

Figures

◀

▶

◀

▶

Back

Close

Full Screen / Esc

Printer-friendly Version

Interactive Discussion



Abstract

A new method for parameterizing the subgrid variations of vertical velocity and cloud droplet number concentration (CDNC) is presented for GCMs. These parameterizations build on top of existing parameterizations that create stochastic subgrid cloud columns inside the GCM grid-cells, which can be employed by the Monte Carlo independent column approximation approach for radiative transfer. The new model version adds a description for vertical velocity in individual subgrid columns, which can be used to compute cloud activation and the subgrid distribution of the number of cloud droplets explicitly. This provides a consistent way for simulating the cloud radiative effects with two-moment cloud microphysical properties defined in subgrid-scale. The primary impact of the new parameterizations is to decrease the CDNC over polluted continents, while over the oceans the impact is smaller. This promotes changes in the global distribution of the cloud radiative effects and might thus have implications on model estimation of the indirect radiative effect of aerosols.

1 Introduction

The interplay between aerosols and clouds is regarded as a major uncertainty in climate prediction and modelling. Besides their direct effects on radiation, aerosols can affect the global radiation budget indirectly by acting as condensation nuclei for cloud droplets, which makes clouds and their radiative properties susceptible to changes in the aerosol size distribution and particle properties (Lohmann and Feichter, 2005).

The physical link between aerosol particles and cloud droplet formation in the current paradigm of simulating cloud droplet formation is the vertical velocity of an ascending air parcel, since it affects the saturation ratio of water vapor through adiabatic cooling. The current state-of-the-art cloud activation parameterizations (e.g. Abdul-Razzak and Ghan, 2000; Fountoukis and Nenes, 2005; Ming et al., 2006; Khvorostyanov and Curry, 2009) rely on this assumption and can solve the critical radius for aerosol particles,

ACPD

13, 5477–5507, 2013

Subgrid vertical velocity and cloud microphysics

J. Tonttila et al.

Title Page

Abstract

Introduction

Conclusions

References

Tables

Figures

◀

▶

◀

▶

Back

Close

Full Screen / Esc

Printer-friendly Version

Interactive Discussion



Subgrid vertical velocity and cloud microphysics

J. Tonttila et al.

Title Page

Abstract

Introduction

Conclusions

References

Tables

Figures

◀

▶

◀

▶

Back

Close

Full Screen / Esc

Printer-friendly Version

Interactive Discussion



given the maximum supersaturation using the Koehler equation (Ghan et al., 2011). When aerosol size distribution is known, the critical radius yields the concentration of cloud condensation nuclei (CCN) and, thus, the number of cloud droplets (Abdul-Razzak et al., 1998; Ghan et al., 2011). From the global modelling perspective, one of the long-lived challenges has been constructing a robust representation of the vertical velocity for cloud activation. Turbulent variability of vertical velocity has a strong impact on the number of cloud droplets in stratiform clouds, and it takes place at scales considerably smaller than the, typically, rather large grid-spacing (on the order of 100–200 km) of global general circulation models (GCM). Therefore, parameterizations are needed to account for the subgrid-scale variations of vertical velocity, i.e. the fluctuations of vertical velocity inside the model grid box around the resolved mean value. Several different approaches have been developed for these parameterizations in GCMs (Ghan et al., 1997; Lohmann et al., 1999; Hoose et al., 2010).

In this paper, we present a new approach to account for the subgrid variations in vertical velocity and its implications on cloud droplet number concentration (CDNC) and cloud radiative effects. Our work builds on top of the ECHAM5.5-HAM2 aerosol-climate model which has been augmented with a stochastic cloud generator (SCG; Räisänen et al., 2004) and the Monte Carlo Independent Column Approximation radiation scheme (McICA; Pincus et al., 2003). In operation, the SCG divides a GCM grid-column into an ensemble of cloudy subgrid columns which can be used directly by the McICA radiation scheme. Implementation of the SCG and McICA to ECHAM5 has been documented and evaluated in several studies (Räisänen et al., 2007, 2008; Räisänen and Järvinen, 2010).

Although the SCG can generate horizontally inhomogeneous cloud condensate amount for the subgrid columns, this framework has been constrained by the lack of information on the subgrid variability of CDNC that, until now, has been assumed horizontally homogeneous for GCM grid-cells. The goal of this work is to remove this constraint. When both the cloud condensate amount and CDNC are described in each subgrid column separately, the direct coupling with McICA radiation scheme provides

Subgrid vertical velocity and cloud microphysics

J. Tonttila et al.

Title Page

Abstract

Introduction

Conclusions

References

Tables

Figures

◀

▶

◀

▶

Back

Close

Full Screen / Esc

Printer-friendly Version

Interactive Discussion



a consistent way of representing the cloud radiative effects at subgrid scale without the need to average the subgrid cloud properties back to GCM-scale between the processes. To achieve this goal, a new parameterization for vertical velocity in the subgrid cloudy columns is implemented, and it is coupled with the cloud droplet activation of aerosols and cloud microphysics. While aerosols also influence ice clouds, the current paper focuses on processes involving only warm (i.e. liquid-phase) clouds.

Our work will be presented as follows. Section 2 gives the model description for the ECHAM5.5-HAM2 aerosol-climate model, while Sect. 3 presents the implementation of new parameterized subgrid components and modifications to the model configuration. Simple test runs are performed, for which experimental details are outlined in Sect. 4. Afterwards, results and model evaluation are presented in Sect. 5. Discussion and conclusions are given in Sects. 6 and 7.

2 Model description

Our baseline modelling system comprises the global atmospheric aerosol-climate model ECHAM5.5-HAM2. In ECHAM5.5 (Roeckner et al., 2003, 2006), the model dynamics are described in spectral space with spherical harmonics, while the model physics are calculated in grid-point space. The physical parameterizations in the model, including those representing turbulence, deep convection, stratiform cloud properties, gravity wave drag and surface properties are invoked every timestep. Parameterizations controlling radiation are called every two hours.

HAM2 (Zhang et al., 2012) is an interactive aerosol model that describes the evolution of the atmospheric aerosol population, accounting for five, presumably, most important particle compositions (dust, black carbon, sulphate, organic carbon and sea salt; secondary organic aerosol is described by O'Donnel et al., 2011). The aerosol size distribution is represented by 7 lognormal modes (the M7-module; Vignati et al., 2004). The dynamically described aerosol environment is coupled with the stratiform cloud microphysics scheme in ECHAM5 (Lohmann and Roeckner, 1996; Lohmann et al., 2007),

where cloud droplet activation is described by Abdul-Razzak and Ghan (2000) and autoconversion of cloud droplets to rain is parameterized according to Khairoutdinov and Kogan (2000).

In addition, we have augmented our model configuration with two components: (1) a stochastic cloud generator (SCG; Räisänen et al., 2004) and (2) the Monte Carlo Independent Column Approximation (McICA; Pincus et al., 2003) for radiative transfer. The SCG is a statistical algorithm that creates subgrid-scale columns (referred to as “subcolumns” from here on) to represent inhomogeneous cloud structure (cloud cover and cloud condensate) inside the GCM grid-column. Another difference to the default settings of ECHAM5.5-HAM2 is that the Tompkins (2002) cloud scheme is active in our model. This is essential because statistical information about the subgrid variability of total water mixing ratio is carried within the Tompkins scheme, eventually enabling the generation of the cloudy subcolumns, as described in detail in Räisänen et al. (2007).

The McICA radiation scheme uses the parameterizations by Mlawer et al. (1997) for longwave (LW) radiation, and Fouquart and Bonnel (1980) and Cagnazzo et al. (2007) for shortwave radiation. The scheme operates by drawing random samples from the ensemble of subcolumns created by the SCG, using a different column for each term in the spectral integration.

3 Subgrid vertical velocity and cloud microphysics

3.1 Principle

The stratiform cloud microphysics scheme, comprising prognostic equations for cloud water content and cloud droplet number concentration (CDNC) (Lohmann et al., 2007), is modified following three waypoints: (1) a parameterization for subcolumn vertical velocity w is implemented, (2) the parameterization for cloud droplet activation (Abdul-Razzak and Ghan, 2000) is modified for subcolumns and (3) the key cloud microphysical processes controlling CDNC are treated explicitly in the subcolumn space.

Subgrid vertical velocity and cloud microphysics

J. Tonttila et al.

Title Page

Abstract

Introduction

Conclusions

References

Tables

Figures



Back

Close

Full Screen / Esc

Printer-friendly Version

Interactive Discussion



Subgrid vertical velocity and cloud microphysics

J. Tonttila et al.

Title Page

Abstract

Introduction

Conclusions

References

Tables

Figures

◀

▶

◀

▶

Back

Close

Full Screen / Esc

Printer-friendly Version

Interactive Discussion



A flowchart of the subgrid treatment of warm clouds is given schematically in Fig. 1 where different processes are presented in chronological order starting from the top of the figure. In addition, lines between the processes indicate the scale in which the computations take place: a single thick line describes GCM-scale processes, while thin lines indicate processes operating in the subcolumn space. Starting from the top of Fig. 1, the Tompkins (2002) cloud cover scheme is used to diagnose the GCM-scale cloud fraction, and statistical properties related to the distribution of cloud condensate amount inside the GCM grid-cell. Next, cloudy subcolumns are created by the SCG, based on information provided by the Tompkins (2002) scheme as described in Räisänen et al. (2007). A cloud fraction of 0 or 1 is assigned to each model layer of the subcolumns with condensate amount varying between the subcolumns. This is followed by the diagnosis of the subcolumn cloud-base vertical velocity w by the new parameterization, which is then used to calculate the maximum supersaturation (S^{\max}) for cloud activation. This in turn enables the calculation of CDNC in the cloudy subcolumns. Since the subcolumns are stochastic and re-generated for each timestep, the subcolumn CDNC distribution is treated as a diagnostic property. Prognostic CDNC is retained at GCM-scale as (Lohmann et al., 1999):

$$\frac{\partial N}{\partial t} = Q^{\text{nucl}} - Q^{\text{aut}} - Q^{\text{self}} - Q^{\text{frz}} + Q^{\text{mit}} - Q^{\text{evap}} - Q^{\text{accr}}. \quad (1)$$

Here, and in all subsequent equations, CDNC is denoted as N . Q^{nucl} and Q^{mit} represent source terms due to droplet nucleation and melting of ice particles, respectively. The sink terms are given by Q^{aut} , Q^{self} , Q^{frz} , Q^{evap} and Q^{accr} (autoconversion of cloud droplets to rain, self-collection of cloud droplets, freezing, evaporation and accretion of cloud droplets by rain or snow, respectively). The terms on the right-hand-side of Eq. (1) represent GCM-scale values, although subcolumn-scale properties can be used to compute them. To save computational cost, in addition to cloud activation (Q^{nucl}), only autoconversion (Q^{aut}) is treated explicitly in the subcolumn space, as shown in Fig. 1. These processes comprise most of the non-linearities affecting the CDNC and

are therefore chosen for the explicit subgrid treatment. The remaining processes comprise mostly phase-changes depending on temperature and are thus assumed to affect only the mean of the CDNC in the GCM grid-cell, for which the ensemble of subcolumn CDNC will be adjusted, accordingly. After the cloud microphysical calculations have been completed, the subcolumn values of cloud fraction (0/1), cloud condensate amount and CDNC are employed in the McICA radiation calculations, providing the GCM grid-column mean radiative fluxes for shortwave and longwave radiation. Next, key features related to the subcolumn vertical velocity parameterization, cloud activation and CDNC are presented in more detail.

3.2 Subcolumn parameterization for vertical velocity

A simple Monte Carlo-type sampling is used to diagnose subcolumn vertical velocity for cloud activation $w_{j,k}$ (the indices are used to emphasize subcolumn values – j denotes the subcolumn index and k denotes model level). A probability density function (PDF) is utilized to represent the subgrid-scale variability in w . Instead of integrating the cloud droplet activation over the vertical velocity PDF for a mean CDNC, positive vertical velocity samples are drawn from the PDF, providing cloud-base vertical velocity in each subcolumn inside a GCM grid-cell. The parameterizations for cloud activation commonly assume that supersaturation is produced only by the adiabatic cooling of ascending parcels of air (Ghan et al., 2011), which is why the negative side of the vertical velocity PDF is left unused.

For this paper, a Gaussian PDF is implemented to provide a simple approximation of the vertical velocity PDF shape. The resolved GCM-scale vertical velocity $\langle w \rangle$ is taken as the mean of the PDF (\bar{w}). Lohmann et al. (2007) parameterized the effective vertical velocity for GCM grid-cells as

$$w^{\text{eff}} = \langle w \rangle + 1.33 \sqrt{\text{TKE}} \quad (2)$$

Subgrid vertical velocity and cloud microphysics

J. Tonttila et al.

Title Page

Abstract

Introduction

Conclusions

References

Tables

Figures



Back

Close

Full Screen / Esc

Printer-friendly Version

Interactive Discussion



We will use a similar TKE-term (second term on the right-hand-side in Eq. (2) to parameterize the standard deviation of the vertical velocity PDF (σ_w), so that

$$\sigma_w = C \sqrt{\text{TKE}}, \quad (3)$$

where C is a scaling coefficient. For a direct comparison with the standard model version using GCM-scale cloud microphysics, we match the average magnitude of $w_{j,k}$ from the new parameterization with the magnitude of w^{eff} (Eq. 2). It can be easily shown (Fountoukis et al., 2007; Morales and Nenes, 2010) for a Gaussian distribution with mean at 0 m s^{-1} , that the average vertical velocity over the positive side of the PDF is given by $w^+ \approx 0.79 \sigma_w$. This can serve as a rough estimate in a global climate model, since $\langle w \rangle$ is usually very small. To ensure that $w^{\text{eff}} \approx w^+$, we set $C = 1.33/0.79 = 1.68$. Interpreting w^{eff} simply as the mean over the positive side of the PDF is not necessarily correct, but it serves the purpose for our comparison. However, one should also note that using $C = 1.68$ for σ_w can be viewed unphysical, as it implies that small-scale variations in vertical velocity contain more energy than the TKE. Effects of this assumption will be presented and accounted for later in Sect. 5.3.

We assume that the coupling between vertical velocity and cloud thermodynamics is weak at cloud base of stratiform clouds, similar to Morales and Nenes (2010). Thus, there is no correlation between cloud base vertical velocity and cloud structure.

3.3 Supersaturation and cloud activation

The parameterization for cloud activation (Abdul-Razzak et al., 1998; Abdul-Razzak and Ghan, 2000) has been modified to operate in the subcolumn space. In the parameterization, a balance equation for maximum supersaturation (Leitch et al., 1986) in an ascending parcel of air is solved for individual subcolumns:

$$\frac{dS_{j,k}}{dt} = A(T)w_{j,k} - B(\rho, T) \frac{dq_j^*}{dt} \quad (4)$$

Subgrid vertical velocity and cloud microphysics

J. Tonttila et al.

Title Page

Abstract

Introduction

Conclusions

References

Tables

Figures

◀

▶

◀

▶

Back

Close

Full Screen / Esc

Printer-friendly Version

Interactive Discussion



Subgrid vertical velocity and cloud microphysics

J. Tonttila et al.

Title Page

Abstract

Introduction

Conclusions

References

Tables

Figures

◀

▶

◀

▶

Back

Close

Full Screen / Esc

Printer-friendly Version

Interactive Discussion

Here $S_{j,k}$ denotes water vapour supersaturation in subcolumn j at model level k , A is a function of temperature (T) and B is a function of temperature and pressure (p) (for more detailed view on the solution method, see Abdul-Razzak et al., 1998). The first term on the right-hand-side of Eq. (4) represents the production of supersaturation due to adiabatic cooling as the air parcel is ascending, while the second term represents a sink due to condensation on existing droplets. The condensation rate of water during the activation process is denoted by $\frac{dq_i^*}{dt}$. The subcolumns do not include any perturbation in pressure or temperature from the GCM mean state. Thus, for a given thermodynamic state and aerosol size distribution in the GCM grid-cell, the subcolumn distribution of S^{\max} depends solely on the distribution of w , according to Eq. (4).

The subcolumn distribution of $S_{j,k}^{\max}$ yields the maximum number of newly activated droplets $N_{j,k}^{\text{act}}$ by finding the critical radius for aerosol particles, above which the particles can act as cloud condensation nuclei (CCN) (Ghan et al., 2011). For GCM-scale nucleation rate we use the same assumption as in the default ECHAM5.5-HAM2 (Lohmann et al., 1999):

$$Q_k^{\text{nucl}} = \text{MAX} \left(0, \frac{1}{\Delta t} \left(\langle N^{\text{act}} \rangle_k - \langle N^{\text{old}} \rangle_k \right) \right), \quad (5)$$

where, in this case, N^{old} is the cloud droplet number concentration from the last timestep. The brackets refer to the GCM-scale mean. More specifically, in the sub-column space, the CDNC profiles are constructed from surface upwards. The cloudy portion of a GCM grid-cell can potentially contain both cloud-base and in-cloud subcolumn points. For subcolumns representing a cloud base at a given model level, $N_{j,k}^{\text{act}}$ is assigned as an initial CDNC. For in-cloud subcolumn levels, CDNC is determined by the number of nucleated droplets at their corresponding cloud-base levels according to the adiabatic assumption. However, as implied by Eq. (5), we do not allow nucleation

to decrease the mean CDNC. Thus, the fraction

$$f_k = \text{MAX} \left(1, \frac{\langle N^{\text{old}} \rangle_k}{\langle N^{\text{act}} \rangle_k} \right) \quad (6)$$

is used to adjust $N_{j,k}^{\text{act}}$ in the case $f_k > 1$, i.e. when $\langle N^{\text{act}} \rangle_k < \langle N^{\text{old}} \rangle_k$. This yields the
5 expression for the final subgrid CDNC after nucleation as $N_{j,k} = f_k N_{j,k}^{\text{act}}$.

3.4 Radiative transfer

Radiative transfer is computed using the McICA radiation scheme already implemented
in our ECHAM5 configuration. The subcolumns are sampled randomly for radiation
calculations, which then follow the standard approaches. The setup of McICA follows
10 the CLDS approach in Räisänen et al. (2007). Random sampling of subcolumns is
confined to the cloudy part of the GCM column, while for clear-sky calculations the
GCM columns are assumed horizontally uniform.

4 Experiments

In this section we present configuration details for the model simulations used to evalu-
ate the primary impacts of the new subgrid parameterizations. The model is run for a 5-
15 yr period (2001–2005) in all experiments with climatological sea surface temperatures.
All the simulations are performed with T42L19 resolution and with 30 min timestep.
The SCG framework is set up to use 50 subcolumns for the cloudy portion of the GCM
grid-column. The generalized overlap method (Räisänen et al., 2004) is employed for
20 creating the vertical cloud profiles, with decorrelation length of 2 km for cloud fraction
and 1 km for condensate. Next, each experiment is described more thoroughly. A sum-
mary of the experiments with their key parameters and configuration options is given
in Table 1.

4.1 Experiment REF

The experiment REF serves as the point of reference using the standard configuration of ECHAM5.5-HAM2 with the SCG and McICA radiation scheme active. The simulation includes cloud layers determined by the SCG with subgrid variations in cloud condensate, while CDNC is assumed uniform inside the GCM grid-cell. The subgrid-scale variations in condensate amount are considered for radiative transfer but not for cloud microphysics. Vertical velocity for cloud activation is given by the effective vertical velocity according to Eq. (2) (Lohmann et al., 2007).

4.2 Experiments SUBW, SUBWRT

The most straightforward implementation of the subcolumn cloud microphysical parameterizations is presented in the experiments SUBW and SUBWRT. In these simulations, cloud activation and CDNC are calculated individually in each subcolumn with the newly-implemented subgrid parameterization for vertical velocity. The only difference between SUBW and SUBWRT lies in the values of closure (“tuning”) parameters. SUBW uses identical parameters with REF while SUBWRT is retuned to restore the global mean radiative balance at the top of the atmosphere (TOA). Specifically, the values of the parameters controlling autoconversion (ccraut) and accretion (cauloc) are adjusted.

4.3 Experiments W_ADJ1, W_ADJ2

To investigate the effect of adjusting the width of the vertical velocity PDF, the experiments W_ADJ1 and W_ADJ2 are performed with $\sigma_w = \sqrt{2TKE}$ and $\sigma_w = \sqrt{\frac{2}{3}TKE}$. Like so, W_ADJ1 assumes that all of the turbulent kinetic energy is associated with fluctuations in vertical motion of air, while W_ADJ2 assumes isotropic turbulence. Both of these experiments are otherwise identical to SUBWRT.

ACPD

13, 5477–5507, 2013

Subgrid vertical velocity and cloud microphysics

J. Tonttila et al.

Title Page

Abstract

Introduction

Conclusions

References

Tables

Figures

◀

▶

◀

▶

Back

Close

Full Screen / Esc

Printer-friendly Version

Interactive Discussion



5 Results

The direct impacts on cloud properties due to the subcolumn treatment of cloud microphysics are presented first. Second, the consequent impacts on cloud radiative effects are presented. For a fair comparison with REF, the width of the PDF for w in the experiments SUBW and SUBWRT was deliberately set so that on average, the vertical velocity for cloud activation matches the w^{eff} used in REF. This is indeed the case, as shown in Fig. 2 depicting the lower tropospheric vertical velocity for REF and SUBW: the simulated global mean vertical velocity is almost identical in the two simulations and the local differences are most often below 0.1 ms^{-1} .

5.1 Cloud properties

Global mean cloud parameters averaged over the 5-yr period are summarized in Table 2: the liquid and ice water paths (LWP and IWP, respectively) as well as the all-sky global mean CDNC at cloud top and the total cloud fraction are listed for REF, SUBW and SUBWRT (plus the remaining experiments W_ADJ1 and W_ADJ2, which are discussed later in Sect. 5.3). While the total cloud fraction and IWP show hardly any change, global mean LWP and CDNC at cloud top are substantially smaller in SUBW than in REF. For closer inspection, we present vertically averaged in-cloud properties for the lower troposphere (from surface to 800 hPa), where we expect most of the changes to take place because only parameterizations for warm clouds have been modified. Figure 3a and b illustrate the 5-yr mean lower tropospheric CDNC for the experiments REF and SUBW, respectively, and the difference between the two experiments is given in Fig. 3c. SUBW shows a strong decrease in CDNC over the continents compared to REF, while for marine areas, a slight but widespread decrease is seen. However, parts of the remote Southern Hemisphere marine regions are almost unaffected, and CDNC is even slightly increased in the marine stratocumulus regions of Eastern Pacific and Atlantic oceans. Overall, the global mean CDNC is approximately 26% smaller in SUBW than in REF. Similar results are also seen for the lower tropo-

Title Page

Abstract

Introduction

Conclusions

References

Tables

Figures

◀

▶

◀

▶

Back

Close

Full Screen / Esc

Printer-friendly Version

Interactive Discussion



spheric LWC shown in Fig. 4a–c. As compared to REF, the LWC is globally decreased in SUBW, in accordance with the decrease in LWP shown in Table 2. The strongest decrease again takes place over the continents, with LWC locally up to 50% smaller in SUBW than in REF. The global mean LWC is decreased by 22%.

5 Since the LWP over the oceans is unrealistically low in SUBW (42.4 g m^{-2} as compared with an observed range of $50 - 84 \text{ g m}^{-2}$ used in Lohmann and Ferrachat, 2010), retuning the closure parameters for autoconversion and accretion rates to lower values (ccraut and cauloc, respectively, see Table 1) is necessary. In the retuned experiment SUBWRT, the global mean LWP is similar to that in REF (approximately 51 g m^{-2} , see
10 Table 2) and the mean over oceans in SUBWRT is 56.7 g m^{-2} , which is slightly larger than in REF (54.8 g m^{-2}). Figure 4d and e show the impact of retuning on the lower tropospheric LWC, which is clearly higher in SUBWRT than in SUBW, especially in the marine stratocumulus areas and over midlatitude oceans. However, over several continental regions, LWC is still substantially smaller than in REF. The impact of retuning on CDNC is presented in Fig. 3d, e, where an increase in SUBWRT with respect to SUBW
15 is seen as well. However, the relative effect is smaller than for LWC as the global mean CDNC in SUBWRT is still about 18% smaller than in REF and large regional decreases still appear over the continents.

It is evident that explicit description of subgrid vertical velocity acts primarily to decrease CDNC in our results. In the modified model version, cloud activation is modulated by the interplay between subgrid distribution of vertical velocity and the large-scale cloud condensation nuclei (CCN) environment. It can be argued that vertical velocity is more important than the number of CCN for CDNC in heavily polluted areas because of the competition for cloud water between droplets, while the opposite
20 is true for more pristine regions (Reutter et al., 2009). In polluted areas, samples with small w (i.e. smaller than w^{eff}) dominate the corresponding subcolumn ensemble of the number of activated droplets, because CDNC increases non-linearly with increasing w . Therefore, the average number of activated cloud droplets and, consequently, the GCM-scale mean CDNC is smaller in SUBW than in REF (as seen especially for
25

Subgrid vertical velocity and cloud microphysics

J. Tonttila et al.

[Title Page](#)[Abstract](#)[Introduction](#)[Conclusions](#)[References](#)[Tables](#)[Figures](#)[⏪](#)[⏩](#)[◀](#)[▶](#)[Back](#)[Close](#)[Full Screen / Esc](#)[Printer-friendly Version](#)[Interactive Discussion](#)

continental regions in Fig. 3c), even though the average vertical velocity is similar. In contrast, in the pristine marine areas, most of the CCN, comprising fewer particles, are activated already by rather low vertical velocity at cloud base. Thus, the low end of the spectrum for subcolumn vertical velocity ensemble is not as dominant as it is for the more polluted environment and the resulting mean CDNC is closer to that obtained using w^{eff} (as seen e.g. for southern marine areas in Fig. 3c for SUBW).

Furthermore, our findings regarding LWC are qualitatively similar to the results obtained by Morales and Nenes (2010), who demonstrated that considering the subgrid vertical velocity distribution leads to stronger autoconversion, as compared to using an effective mean vertical velocity. This can be explained by interaction with the low end of the subgrid CDNC ensemble, since the autoconversion rate e.g. in Khairoutdinov and Kogan (2000) scales as $\text{CDNC}^{-1.79}$. The coupling between subcolumn CDNC and the parameterized autoconversion yields the depleted LWC seen in the experiment SUBW (Fig. 4b, c), which was restored by retuning in SUBWRT (Fig. 4d, e).

5.2 Radiative balance

Table 3 summarizes the radiative impacts between the model experiments. Absolute values for the net total radiative budget at TOA, and the longwave (LW) and shortwave (SW) cloud radiative effects (CRE) are listed for REF, while for SUBW and SUBWRT the difference with respect to REF is presented. Introducing the subcolumn vertical velocity and CDNC deflects the total radiative budget off balance by 3.6 W m^{-2} , for the most part due to reduction in CDNC and subsequent removal of cloud condensate. Overall, the total radiative budget balances at quite low levels of outgoing longwave radiation (OLR) and net shortwave flux at TOA (approximately 231 W m^{-2} for REF), regardless of the model configuration. This was also found for ECHAM5.3 (Räisänen and Järvinen, 2010) and was ascribed to low clear-sky OLR and too strong shortwave cloud radiative effects (CRE). In addition, in the current paper, a persistent feature of quite high total cloud fraction of over 70% is seen (Table 2), which contributes to the CRE and the global radiation budget in general.

Subgrid vertical velocity and cloud microphysics

J. Tonttila et al.

Title Page

Abstract

Introduction

Conclusions

References

Tables

Figures

◀

▶

◀

▶

Back

Close

Full Screen / Esc

Printer-friendly Version

Interactive Discussion



Subgrid vertical velocity and cloud microphysics

J. Tonttila et al.

Title Page

Abstract

Introduction

Conclusions

References

Tables

Figures

◀

▶

◀

▶

Back

Close

Full Screen / Esc

Printer-friendly Version

Interactive Discussion



Considering the CRE at TOA, the largest differences are seen for SW radiation. Figure 5a and b show the difference in SW CRE for SUBW and SUBWRT with respect to REF. While SW CRE in SUBW is weaker (i.e. less negative) than in REF almost globally in response to the smaller CDNC, SUBWRT shows weaker SW CRE mainly over the continental regions of South-East Asia and the eastern parts of North and South America. In contrast, a slight preference for stronger SW CRE is seen over the mid-latitude oceans and Eastern Pacific stratocumulus regions off the coasts of North and South America, as well as in the Atlantic off the coast of Namibia. The direct impact in SUBW is thus to weaken the SW CRE by 4.08 W m^{-2} from the -54.47 W m^{-2} seen in REF in terms of the global mean (Table 3). In SUBWRT, this is compensated by retuning, after which the difference to REF is -0.41 W m^{-2} .

Differences in LW CRE at TOA between SUBW/SUBWRT and REF are shown in Fig. 5c, d. In both cases, differences are seen mostly in tropical latitudes. The global mean stays reasonably close to the recently published estimate of 26.6 W m^{-2} (Stephens et al., 2012) in all our experiments. As shown in Table 3, the strongest LW CRE occurs in REF (27.29 W m^{-2}) while the weakest value is seen for SUBW (26.74 W m^{-2} , in correlation with the lowest LWP).

5.3 Sensitivity to vertical velocity distribution width

We consider the effect of adjusting σ_w , i.e. the magnitude of vertical velocity fluctuations, by comparing the experiments W_ADJ1 and W_ADJ2 with SUBWRT. Table 2 shows that smaller σ_w decreases the global mean cloud top CDNC as well as the LWC. The same is true for the lower tropospheric CDNC in the two experiments, which, along with the difference with respect to SUBWRT, is presented in Fig. 6a–d. The lower tropospheric CDNC in W_ADJ1 is on average 9.76 cm^{-3} smaller than in SUBWRT. The corresponding difference in W_ADJ2 is -27.69 cm^{-3} . Figure 6e–h show the results for lower tropospheric LWC, which is, subsequently, only slightly decreased in W_ADJ1 with respect to SUBWRT (by 3.39 mg kg^{-1}). Again, in W_ADJ2, the decrease is larger (by 15.31 mg kg^{-1}).

Figure 7 shows the impact of adjusted σ_w on longwave and shortwave CRE. The global mean impacts on LW CRE are minor. The SW CRE for W_ADJ1 and W_ADJ2 are weaker (less negative) than that for SUBWRT, by 0.69 W m^{-2} and 2.88 W m^{-2} , respectively. While only local anomalies are seen over the tropical oceans in both W_ADJ1 and W_ADJ2 for LW CRE, SW CRE shows more widespread differences with largest increases in the marine stratocumulus regions off the western coasts of South-America and Africa. Overall, the impacts on cloud radiative properties due to adjusting the vertical velocity magnitude are more concentrated over the oceans, compared to the effects of implementing the subgrid parameterizations.

6 Discussion

Explicit description of subgrid variability of vertical velocity and CDNC introduces notable differences compared to the existing implementation of McICA radiation and the stochastic cloud generator in ECHAM5.5-HAM2. The subcolumn approach allows the model to account for non-linearities related to subgrid variability not only in individual processes, such as cloud activation, but also in the interactions between different processes.

Gaussian PDF has been used extensively to simulate the small scale variations in vertical velocity (e.g. Ghan et al., 1997) and was also employed in this study. However, we speculate that more careful consideration of the characteristics of the PDF might be important for boundary layer clouds. Perhaps the most obvious such characteristic is the skewness: non-symmetrical vertical velocity PDF shapes in the boundary layer have been observed in measurements and model simulations (Moeng et al., 1990; Guo et al., 2008; Ghate et al., 2010; Lenschow et al., 2012). Our implementation of the subcolumn vertical velocity parameterization allows the PDF to be easily adjusted through the use of look-up tables. Although left outside the scope of the current paper, experiments with skewed vertical velocity distributions are part of our future plans.

Title Page

Abstract

Introduction

Conclusions

References

Tables

Figures

◀

▶

◀

▶

Back

Close

Full Screen / Esc

Printer-friendly Version

Interactive Discussion



Subgrid vertical velocity and cloud microphysics

J. Tonttila et al.

Title Page

Abstract

Introduction

Conclusions

References

Tables

Figures

◀

▶

◀

▶

Back

Close

Full Screen / Esc

Printer-friendly Version

Interactive Discussion



Since the effects of the subcolumn cloud activation and autoconversion on CDNC and LWC were found to vary quite strongly across different regions with different aerosol characteristics, it is possible that these effects will induce perturbations in the model estimates of the indirect aerosol effects on radiation. The evaluation of the new model version should therefore be extended by exposing the model to pre-industrial aerosol emission inventories and, perhaps, to future emission scenarios. Moreover, the McICA radiation scheme, as well as the standard radiation scheme in ECHAM5.5, includes an assumed minimum CDNC of 40cm^{-3} , which is applied to all cloudy sub-columns in our model. It has been shown that this assumption may induce artefacts to the model representation of the indirect aerosol effects (Hoose et al., 2009). We too recognise this as a possible caveat especially regarding the subcolumns, as it might artificially smooth out a part of the subgrid variability in the cloud radiative effects.

7 Summary

This paper reported the implementation of subgrid vertical velocity parameterization and subgrid versions of cloud microphysical parameterizations describing processes such as the cloud droplet activation and autoconversion of cloud droplets to rain. Vertical velocity and cloud properties are calculated using stochastically generated cloudy subgrid columns, which can be directly applied by the McICA radiation scheme included in the model. This enables the model to account for the inherent non-linearities in the entire process chain from defining non-uniform cloud properties to calculating radiative fluxes at subgrid scale.

The brief model evaluation using the new subcolumn parameterizations revealed interesting effects on the interactions between different cloud processes. With the sub-column vertical velocity parameterization and thus subgrid cloud activation switched on, CDNC was decreased especially over continental areas with high aerosol particle concentration. The decreased CDNC together with the non-linearity related to its sub-grid variability induced stronger autoconversion of cloud water to rain, which resulted in

decreased global mean LWC. Retuning the model closure parameters increased LWP back to the observed range, but a decrease in CDNC was seen even after retuning. With the globally and regionally varying effects on CDNC and LWC, the new model version shows the importance of considering the small-scale variability of the two-moment cloud microphysical properties together with radiative transfer more explicitly than what has most often been done in the context of traditional parameterizations for global models.

Acknowledgements. This work has been supported by the Academy of Finland (project number 127210).

References

- Abdul-Razzak, H. and Ghan, S. J.: A parameterization of aerosol activation. 2. Multiple aerosol types, *J. Geophys. Res.*, 105, 6837–6844, 2000. 5478, 5481, 5484
- Abdul-Razzak, H., Ghan, S. J., and Rivera-Carpio, C.: A parameterization of aerosol activation. 1. Single aerosol type, *J. Geophys. Res.*, 103, 6123–6131, 1998. 5479, 5484, 5485
- Cagnazzo, C., Manzini, E., Giorgetta, M. A., Forster, P. M. De F., and Morcrette, J. J.: Impact of an improved shortwave radiation scheme in the MAECHAM5 General Circulation Model, *Atmos. Chem. Phys.*, 7, 2503–2515, doi:10.5194/acp-7-2503-2007, 2007. 5481
- Fouquart, Y. and Bonnel, B.: Computations of solar heating of the Earth’s atmosphere: a new parameterization, *Beitr. Phys. Atmos.* 53, 35–62, 1980. 5481
- Fountoukis, C. and Nenes, A.: Continued development of a cloud droplet formation parameterization for global climate models, *J. Geophys. Res.*, 110, D11212, doi:10.1029/2004JD005591, 2005. 5478
- Fountoukis, C., Nenes, A., Meskhidze, N., Bahreini, R., Conant, W. C., Jonsson, H., Murphy, S., Sorooshian, A., Varutbangkul, V., Brechtel, F., Flagan, R. C., and Seinfeld, J. H.: Aerosol-cloud drop concentration closure for clouds sampled during the International Consortium for Atmospheric Research on Transport and Transformation 2004 campaign, *J. Geophys. Res.*, 112, D10S30, doi:10.1029/2006JD007272, 2007. 5484
- Ghan, S. J., Leung, L. R., and Easter, R. C.: Prediction of cloud droplet number in a general circulation model, *J. Geophys. Res.*, 102, 21777–21794, 1997. 5479, 5492

Subgrid vertical velocity and cloud microphysics

J. Tonttila et al.

Title Page

Abstract

Introduction

Conclusions

References

Tables

Figures



Back

Close

Full Screen / Esc

Printer-friendly Version

Interactive Discussion



Subgrid vertical velocity and cloud microphysics

J. Tonttila et al.

Title Page

Abstract

Introduction

Conclusions

References

Tables

Figures

◀

▶

◀

▶

Back

Close

Full Screen / Esc

Printer-friendly Version

Interactive Discussion



Ghan, S. J., Abdul-Razzak, H., Nenes, A., Ming, Y., Liu, X., Ovchinnikov, M., Shipway, B., Meskhidze, N., Xu, J., and Shi, X.: Droplet nucleation: physically-based parameterizations and comparative evaluation, *J. Adv. Model. Earth Syst.*, 3, M10001, doi:10.1029/2011MS000074, 2011.

5 Ghate, V. P., Albrecht, B. A., and Kollias, P.: Vertical velocity structure of nonprecipitating continental boundary layer stratocumulus clouds, *J. Geophys. Res.*, 115, D13204, doi:10.1029/2009JD013091, 2010. 5479, 5483, 5485

Guo, H., Liu, Y., Daum, P. H., Senum, G. I., and Tao, W.-K.: Characteristics of vertical velocity in marine stratocumulus: comparison of large eddy simulations with observations, *Environ. Res. Lett.*, 3, 045020, doi:10.1088/1748-9326/3/4/045020, 2008. 5492

10 Hoose, C., Kristjansson, J. E., Iversen, T., Kirkevåg, A., Seland, Ø, and Gettelman, A.: Constraining cloud droplet number concentration in GCMs suppresses the aerosol indirect effect, *Geophys. Res. Lett.*, 36, L12807, doi:10.1029/2009GL038568, 2009. 5492

15 Hoose, C., Kristjansson, J. E., Arabas, S., Boers, R., Pawlowska, H., Puygrenier, V., Siebert, H., and Thouron, O.: Parameterization of in-cloud vertical velocities for cloud droplet activation in coarse-grid models: analysis of observations and cloud resolving model results. Proceedings of the 13th AMS Conference on Atmospheric Radiation, Portland, OR, USA, 28 June–2 July 2010. 5493

20 Khairoutdinov, M. and Kogan, Y.: A new cloud physics parameterization in a Large-Eddy Simulation model of marine stratocumulus, *Mon. Weather Rev.*, 128, 229–243, 2000. 5479

Khvorostyanov, V. I. and Curry, J.: Parameterization of cloud drop activation based on analytical asymptotic solutions to the supersaturation equation, *J. Atmos. Sci.*, 66, 1905–1925, 2009. 5481, 5490

25 Leaitch, W. R., Strapp, J. W., and Isaac, G. A.: Cloud droplet nucleation and cloud scavenging of aerosol sulphate in polluted atmospheres, *Tellus B*, 38, 328–344, 1986. 5478 5484

Lenschow, D. H., Lothon, M., Mayor, S. D., Sullivan, P. P., and Canut, G.: A comparison of higher-order vertical velocity moments in the convective boundary layer from lidar with in situ measurements and large-eddy simulation, *Bound.-Lay. Meteorol.*, 143, 107–123, doi:10.1007/s10546-011-9615-3, 2012. 5492

30 Lohmann, U. and Feichter, J.: Global indirect aerosol effects: a review, *Atmos. Chem. Phys.*, 5, 715–737, doi:10.5194/acp-5-715-2005, 2005. 5478

Subgrid vertical velocity and cloud microphysics

J. Tonttila et al.

Title Page

Abstract

Introduction

Conclusions

References

Tables

Figures

◀

▶

◀

▶

Back

Close

Full Screen / Esc

Printer-friendly Version

Interactive Discussion



Lohmann, U. and Ferrachat, S.: Impact of parametric uncertainties on the present-day climate and on the anthropogenic aerosol effect, *Atmos. Chem. Phys.*, 10, 11373–11383, doi:10.5194/acp-10-11373-2010, 2010. 5489

Lohmann, U. and Roeckner, E.: Desing and performance of a new cloud microphysics scheme developed for the ECHAM general circulation model, *Clim. Dynam.*, 12, 557–572, 1996. 5480

Lohmann, U., Feichter, J., Chuang, C. C., and Penner, J. E.: Prediction of the number of cloud droplets in the ECHAM GCM, *J. Geophys. Res.*, 104, 9169–9198, 1999. 5479, 5482, 5485

Lohmann, U., Stier, P., Hoose, C., Ferrachat, S., Kloster, S., Roeckner, E., and Zhang, J.: Cloud microphysics and aerosol indirect effects in the global climate model ECHAM5-HAM, *Atmos. Chem. Phys.*, 7, 3425–3446, doi:10.5194/acp-7-3425-2007, 2007. 5480, 5481, 5483, 5487, 5498

Ming, Y., Ramaswamy, V., Donner, L. J., and Phillips, V. T. J.: A new parameterization of cloud droplet activation applicable to general circulation models, *J. Atmos. Sci.*, 63, 1348–1356, 2006. 5478

Mlawer, E. J., Taubman, S. J., Brown, P. D., Iacono, M. J., and Clough, S. A.: Radiative transfer for inhomogeneous atmospheres: RRTM, a validated correlated-k model for the longwave, *J. Geophys. Res.*, 102, 16663–16682, 1997. 5481

Moeng, C.-H. and Rotunno, R.: Vertical-velocity skewness in the buoyancy-driven boundary layer, *J. Atmos. Sci.*, 47, 1149–1161, 1990. 5492

Morales, R. and Nenes, A.: Characteristic updrafts for computing distribution averaged cloud droplet number and stratocumulus cloud properties, *J. Geophys. Res.*, 115, D18220, doi:10.1029/2009JD013233, 2010. 5484, 5490

O'Donnell, D., Tsigaridis, K., and Feichter, J.: Estimating the direct and indirect effects of secondary organic aerosols using ECHAM5-HAM, *Atmos. Chem. Phys.*, 11, 8635–8659, doi:10.5194/acp-11-8635-2011, 2011. 5480

Pincus, R., Barker, H. W., and Morcrette, J.-J.: A fast, flexible, approximate technique for computing radiative transfer in inhomogeneous cloud fields, *J. Geophys. Res.*, 108, doi:10.1029/2002JD003322, 2003. 5479, 5481

Reutter, P., Su, H., Trentmann, J., Simmel, M., Rose, D., Gunthe, S. S., Wernli, H., Andreae, M. O., and Pöschl, U.: Aerosol- and updraft-limited regimes of cloud droplet formation: influence of particle number, size and hygroscopicity on the activation of cloud condensation nuclei (CCN), *Atmos. Chem. Phys.*, 9, 7067–7080, doi:10.5194/acp-9-7067-2009, 2009. 5489

Subgrid vertical velocity and cloud microphysics

J. Tonttila et al.

Title Page

Abstract

Introduction

Conclusions

References

Tables

Figures

◀

▶

◀

▶

Back

Close

Full Screen / Esc

Printer-friendly Version

Interactive Discussion



- Roeckner, E., Bäuml, G., Bonaventura, L., Brokopf, R., Esch, M., Giorgetta, M., Hagemann, S., Kirchner, I., Koernblueh, L., Manzini, E., Rhodin A., Schlese, U., Schulzweida, U., and Tompkins, A.: The atmospheric general circulation model ECHAM5. Part I: model description. Rep. 349, Max Planck Institute for Meteorology, Hamburg, Germany, 127 pp., 2003. 5480
- 5 Roeckner, E., Brokopf, R., Esch, M., Giorgetta, M., Hagemann, S., Koernblueh, L., Manzini, E., Schlese, U., and Schulzweida, U.: Sensitivity of simulated climate to horizontal and vertical resolution in the ECHAM5 atmosphere model, *J. Climate*, 19, 3771–3791, 2006. 5480
- Räisänen, P., Barker, H. W., Khairoutdinov, M. F., Li, J., and Randall, D. A.: Stochastic generation of subgrid-scale cloudy columns for large-scale models, *Q. J. Roy. Meteorol. Soc.*, 130, 2047–2067, 2004. 5479, 5481, 5486
- 10 Räisänen, P., Järvenoja, S., Järvinen, H., Giorgetta, M., Roeckner, E., Jylhä, K., and Ruosteenoja, K.: Tests of Monte Carlo Independent Column Approximation in the ECHAM5 atmospheric GCM, *J. Climate*, 20, 4995–5011, 2007. 5479, 5481, 5482, 5486
- Räisänen, P., Järvenoja, S., and Järvinen, H.: Noise due to Monte Carlo independent-column approximation: short-term and long-term impacts in ECHAM5, *Q. J. Roy. Meteorol. Soc.*, 134, 481–495, doi:10.1002/qj.231, 2008. 5479
- 15 Räisänen, P. and Järvinen, H.: Impact of cloud and radiation scheme modifications on climate simulated by the ECHAM5 atmospheric GCM, *Q. J. Roy. Meteorol. Soc.*, 136, 1733–1752, doi:10.1002/qj.674, 2010. 5479, 5490
- 20 Stephens, G. L., Li, J., Wild, M., Clayson, C. A., Loeb, N., Kato, S., L'Ecuyer, T., Stackhouse Jr, P. W., Lebsock, M., and Andrews, T.: An update on earth's energy balance in light of the latest global observations, *Nat. Geosci.*, 5, 691–696, doi:10.1038/NGEO1580, 2012. 5491
- Tompkins, A. M.: A prognostic parameterization for the subgrid-scale variability of water vapor and clouds in large-scale models and its use to diagnose cloud cover, *J. Atmos. Sci.*, 59, 1917–1942, 2002. 5482
- 25 Vignati, E., Wilson, J., and Stier, P.: M7: an efficient size-resolved aerosol microphysics module for large-scale aerosol transport models, *J. Geophys. Res.*, 109, D22202, doi:10.1029/2003JD004485, 2004. 5480
- Zhang, K., O'Donnell, D., Kazil, J., Stier, P., Kinne, S., Lohmann, U., Ferrachat, S., Croft, B., Quaas, J., Wan, H., Rast, S., and Feichter, J.: The global aerosol-climate model ECHAM-HAM, version 2: sensitivity to improvements in process representations, *Atmos. Chem. Phys.*, 12, 8911–8949, doi:10.5194/acp-12-8911-2012 2012. 5480
- 30

Subgrid vertical velocity and cloud microphysics

J. Tonttila et al.

Table 1. List of experiments indicating the key configuration details. SGW refers to the subgrid treatment of vertical velocity and cloud activation, while the column labelled as w shows details of the vertical velocity treatment. The terms “ccraut” and “cauloc” refer to model closure parameters on autoconversion rate and accretion, respectively. See text for further description.

Experiment	SGW	w	ccraut	cauloc
REF	No	Lohmann et al. (2007)	7	3
SUBW	Yes	$\sigma_w = 1.68\sqrt{\text{TKE}}$	7	3
SUBWRT	Yes	$\sigma_w = 1.68\sqrt{\text{TKE}}$	4	2
W_ADJ1	Yes	$\sigma_w = \sqrt{2\text{TKE}}$	4	2
W_ADJ2	Yes	$\sigma_w = \sqrt{\frac{2}{3}\text{TKE}}$	4	2

Title Page

Abstract

Introduction

Conclusions

References

Tables

Figures

◀

▶

◀

▶

Back

Close

Full Screen / Esc

Printer-friendly Version

Interactive Discussion



Subgrid vertical velocity and cloud microphysics

J. Tonttila et al.

Table 2. Global mean cloud properties: LWP and IWP are for liquid and ice water paths (g m^{-2}) and C_{tot} is the total cloud fraction [0, 1]. CDNC at cloud top is the all-sky mean value for warm clouds over all timesteps (cm^{-3}).

Experiment	LWP	IWP	CDNC at cloud top	C_{tot}
REF	50.71	7.05	21.48	0.720
SUBW	38.30	6.95	16.08	0.712
SUBWRT	50.87	7.08	18.57	0.722
W_ADJ1	49.27	7.06	17.27	0.721
W_ADJ2	44.78	7.06	12.99	0.717

[Title Page](#)
[Abstract](#)
[Introduction](#)
[Conclusions](#)
[References](#)
[Tables](#)
[Figures](#)
[◀](#)
[▶](#)
[◀](#)
[▶](#)
[Back](#)
[Close](#)
[Full Screen / Esc](#)
[Printer-friendly Version](#)
[Interactive Discussion](#)


Subgrid vertical velocity and cloud microphysics

J. Tonttila et al.

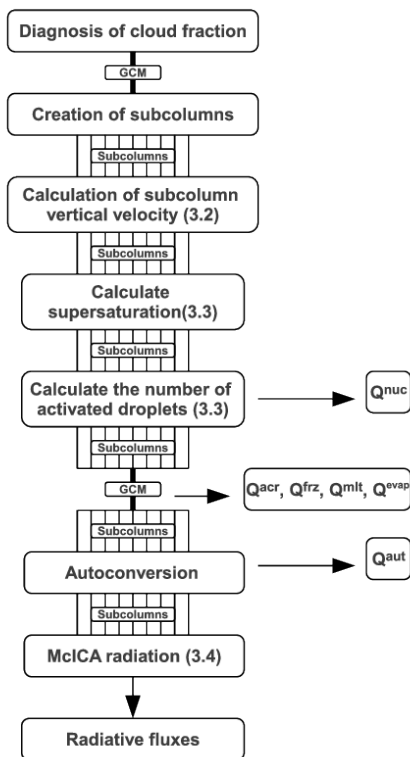


Fig. 1. Schematic description of the work-flow in the new model version with subgrid treatment for vertical velocity and cloud microphysical properties. Thick black lines labelled as “GCM” refer to GCM grid-scale computation, while thin lines labelled as “subcolumns” refer to subgrid representation of processes. Arrows describe the most important outputs from the parameterized processes (all given in GCM grid-scale). Numbers next to some of the processes refer to the section of this paper giving further details.

Title Page

Abstract

Introduction

Conclusions

References

Tables

Figures

◀

▶

◀

▶

Back

Close

Full Screen / Esc

Printer-friendly Version

Interactive Discussion



Subgrid vertical velocity and cloud microphysics

J. Tonttila et al.

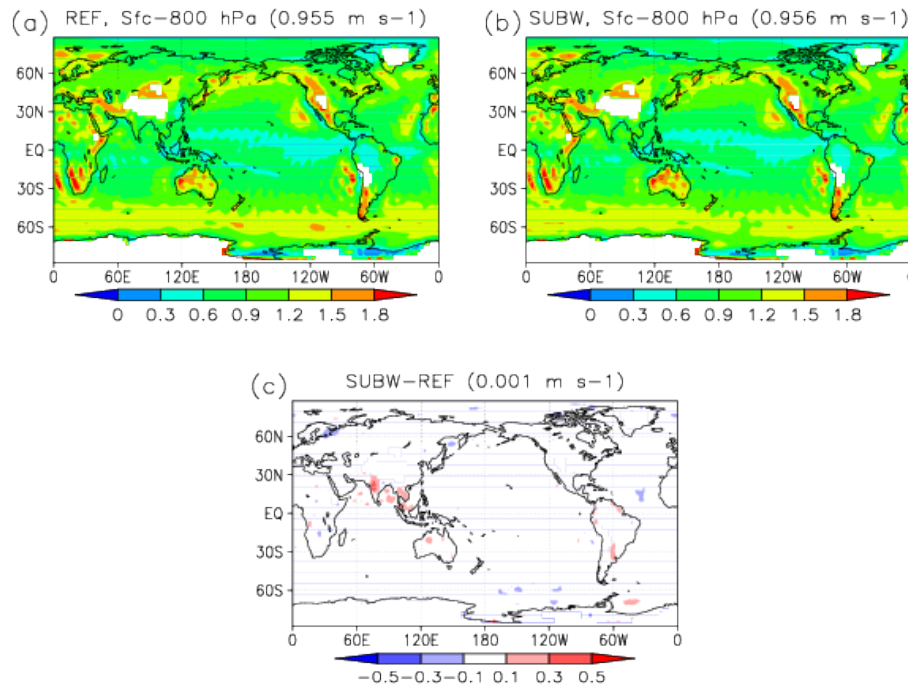


Fig. 2. Annual mean vertical velocity (m s^{-1}) for cloud activation averaged from surface to the 800 hPa pressure level: **(a)** REF, **(b)** SUBW and **(c)** the difference SUBW–REF. Global mean values are indicated in parenthesis.

Subgrid vertical velocity and cloud microphysics

J. Tonttila et al.

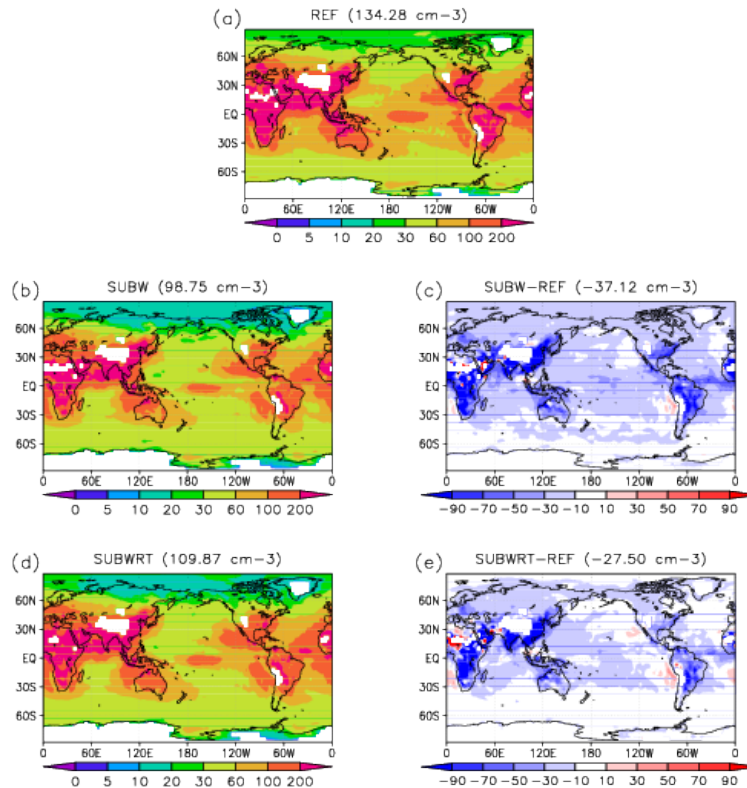


Fig. 3. Annual mean CDNC (cm^{-3}) averaged from surface to the 800 hPa pressure level: **(a)** REF, **(b)** SUBW, **(c)** the difference SUBW-REF, **(d)** SUBWRT, and **(e)** the difference SUBWRT-REF.

Title Page

Abstract

Introduction

Conclusions

References

Tables

Figures

◀

▶

◀

▶

Back

Close

Full Screen / Esc

Printer-friendly Version

Interactive Discussion



Subgrid vertical velocity and cloud microphysics

J. Tonttila et al.

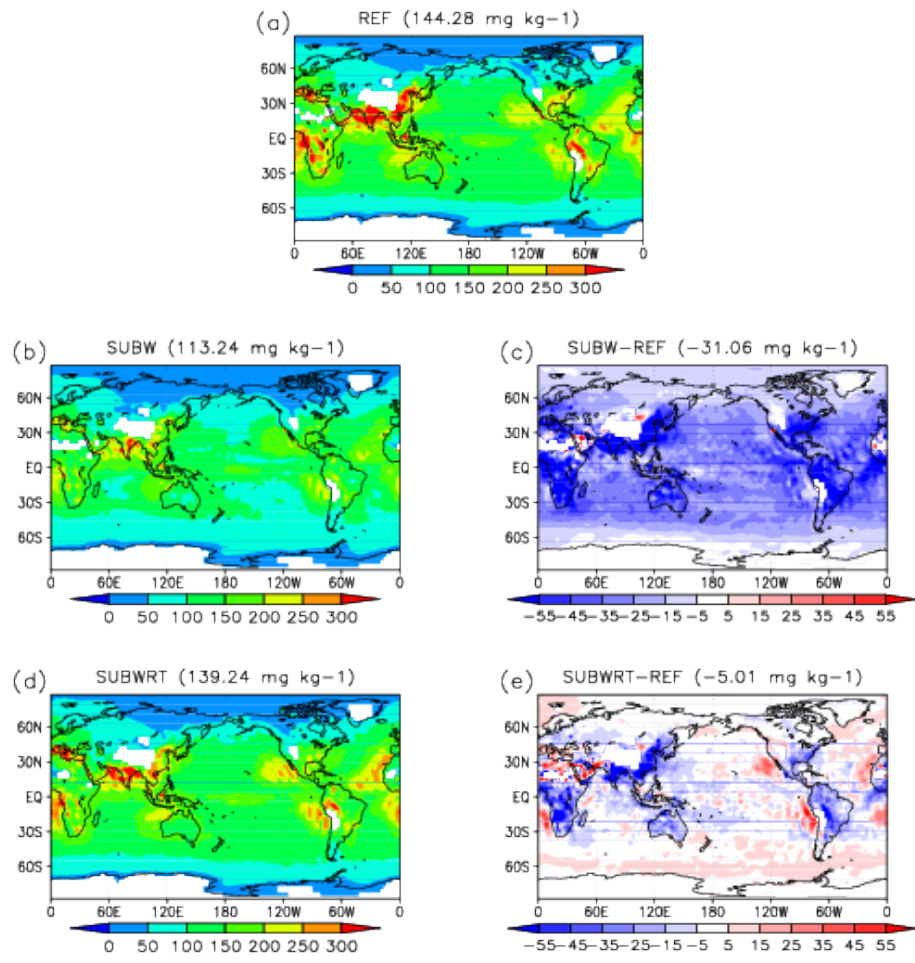


Fig. 4. Same as Fig. 3 but for LWC (mg kg⁻¹).

Title Page

Abstract Introduction

Conclusions References

Tables Figures

◀ ▶

◀ ▶

Back Close

Full Screen / Esc

Printer-friendly Version

Interactive Discussion



Subgrid vertical velocity and cloud microphysics

J. Tonttila et al.

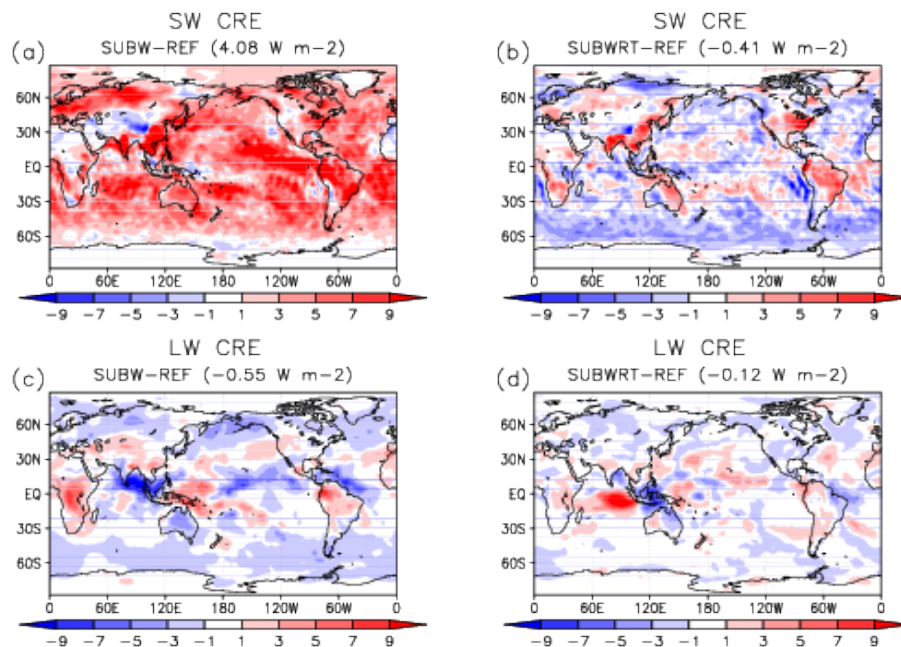


Fig. 5. Difference in annual mean TOA shortwave cloud radiative effects (W m^{-2}) between **(a)** SUBW and REF, and **(b)** SUBWRT and REF. Differences for longwave CRE are given similarly in panels **(c)** and **(d)**.

Title Page

Abstract

Introduction

Conclusions

References

Tables

Figures

◀

▶

◀

▶

Back

Close

Full Screen / Esc

Printer-friendly Version

Interactive Discussion



Subgrid vertical velocity and cloud microphysics

J. Tonttila et al.

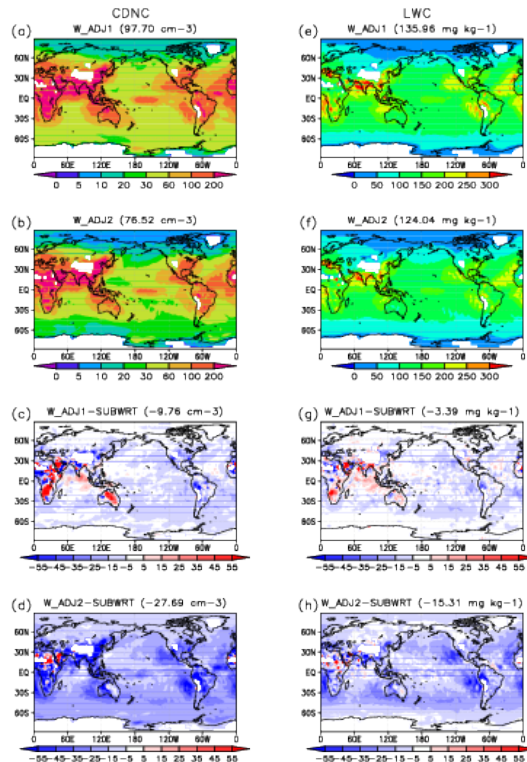


Fig. 6. Effects of adjusting the vertical velocity distribution width on annual mean CDNC (cm^{-3}) and LWC (mg kg^{-1}) averaged from surface to the 800 hPa pressure level. **(a)** and **(b)**: CDNC for the experiments W_ADJ1 and W_ADJ2. **(c)** and **(d)**: The difference with respect to SUBWRT for W_ADJ1 and W_ADJ2. Panels **(e–h)** are the same as **(a–d)**, but for LWC.

Title Page

Abstract

Introduction

Conclusions

References

Tables

Figures

◀

▶

◀

▶

Back

Close

Full Screen / Esc

Printer-friendly Version

Interactive Discussion



Subgrid vertical velocity and cloud microphysics

J. Tonttila et al.

Title Page

Abstract

Introduction

Conclusions

References

Tables

Figures

◀

▶

◀

▶

Back

Close

Full Screen / Esc

Printer-friendly Version

Interactive Discussion

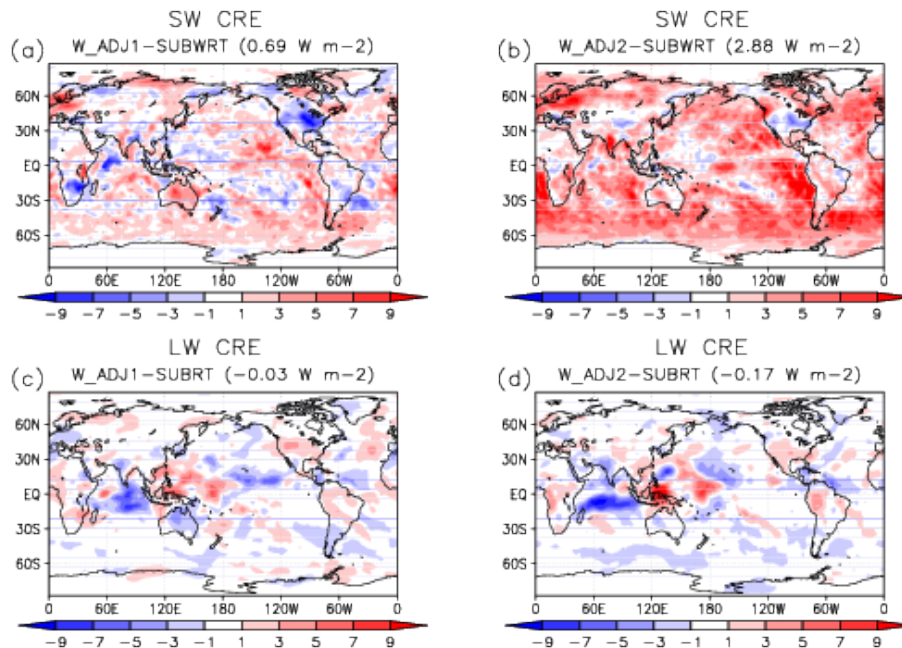


Fig. 7. Difference in annual mean TOA shortwave cloud radiative effects (W m^{-2}) between **(a)** W_ADJ1 and SUBWRT, and **(b)** W_ADJ2 and SUBWRT. Differences in longwave CRE are given similarly in panels **(c)** and **(d)**.